Evaluation of Tilting Pad Thrust Bearing Stiffness And Damping Characteristics in Vertical Machines

D. V. Srikanth
Member

K. K. Chaturvedi
Member

A. Chenna Keshav Reddy
Non-Member

ABSTRACT

Tilting pad thrust bearings are designed to transfer high axial loads from rotating shafts with minimum power loss. In the present paper, formulation of Reynold's equation for the bearing is done in two dimensions (planar). A Finite Difference Method is used to convert the terms of the Reynolds equation in to a set of simultaneous linear algebraic equations. A solution procedure for finding value of the pressure in the oil film is described. Numerical integration of the pressure values gives the load distribution.

Subsequently, the study of dynamic stiffness and damping characteristics of the bearing is done by varying the value of the oil film thickness and introducing vertical velocity in the runner.

Large thrust bearing behavior in a realistic configuration allowing sufficient parameter variation to check the fidelity of this analytical model is to be developed. This data is useful as an input for rotor dynamics studies of the vertical rotors. The agreement supports the fidelity and accuracy of the software package and its continued use in analysis and design.

INTRODUCTION

Each bearing consists of a series of pads supported in a carrier. ring as shown in Fig.1; each pad is free to tilt so that it creates a self-sustaining hydrodynamic film. There are two main types of dynamic condition common to all bearings as studied in [1]. One condition is concerned with dynamically loaded bearings such as in internal combustion engines in which the load is constantly changing in magnitude and direction.

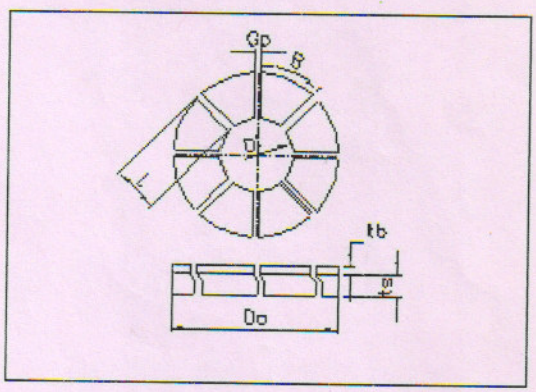

FIG.1 Geometry of the thrust pad

The other dynamic condition is when acceleration occurs. This takes place when a sudden space change occurs in an operating turbine. A knowledge of how the oil film builds up as the rotational speed, increases is of vital importance with a view to promoting the rapid formation of a thick oil film separating the two bearing components.

To date there has been a minimal effort to evaluate the transient response of a slider bearing undergoing acceleration in the tangential direction. Unsteady operation is one of the primary mechanisms of failure in a fluid bearing.

The transient response of the thrust bearing has been studied numerically as in [2] and of greatest interest is the mode of boundary layer formation and the subsequent development of the pressure in the supporting film. The supporting film is found to be fully developed in the course of a few milliseconds. The most interesting discovery was that in a titling pad bearing the

2. The lubricant is incompressible.
3. The lubricant is Newtonian.
4. Flow in the convergent wedge is laminar.
5. Pressure and shear effects on the viscosity are negligible.
6. Variation of the specific heat and density with pressure is negligible.
7. Wherever the oil film becomes divergent due to crowning or thermoelastic distortion, cavitation is taken into account, by making pressure equal to zero, wherever its value is negative.

DYNAMIC COEFFFICIENTS

a)The damping coefficient , C_z , is calculated using

$$C_z = \Delta W / \Delta V$$

The subscript 'z' refers to the vertical direction of motion, orthogonal to the direction of the applied forces. Where W is the component of force causing displacement, measured in N, and V is the vertical velocity, measured in m/s.

The damping of a system is its ability to absorb energy and is measured in N.sec/m.

b)The stiffness coefficient, K_z , was calculated using

$$K_z = \Delta W / \Delta h_o$$

The stiffness of a material or system is its ability to resist deformation by an applied force and it is measured as the force required to produce a displacement of one linear unit. In this case, stiffness was measured in N/m .

CALCULATION OF DYNAMIC COEFFICIENTS

The stiffness and damping characteristics are calculated for 1) Author's data and 2) Yuan's data (Case 1) as in [5] as listed in Table 1. Spring arrangement of pad is shown in Fig. 3. Initially we are taking the values of a and ho and by substituting these values in the equation of the shape of the oil film we gradient film thickness coefficients.

Table 1: Thrust Bearing Geometry

	Yuan's data (Case 1)	Author's data
Outer Diameter (m)	1.168	1.275
Inner Diameter(m)	0.711	0.75
Number of Pads	12	6
Thickness (mm)	41.1	--
Groove width(mm)	52.3	84
Number of Springs	15	-
Operating Conditions		
Load (MN)	2.124	--
Rotational speed (rads/s)	52.4	14.28
Oil pot temperature (° C)	70	40
Oil properties		
ISO grade	46	--
γ (cSt) at 40 ° C	48	73
γ (cSt) at 100 ° C	6.70	10.7
ρ (g/m) at 15 ° C	0.873	0.861

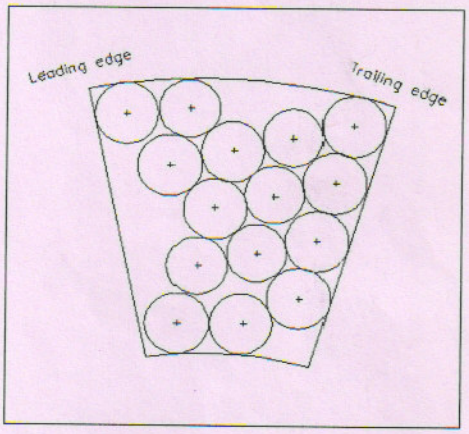

Fig. 3 Spring arrangement of pad

RESULTS AND DISCUSSIONS :

By substituting these values of gradient film thickness in modified Reynold's equation we get pressure at each node. Fig.4 shows 3-D pressure distribution in the oil film of a flat pad. By numerical integration to these pressure points we get the load .The values of *W* and *V* are varied from +10% to -10% and the difference of these values are taken ie. ΔW *and* ΔV . Table 2 shows damping coefficients calculated for the author's parameters.

TABLE-2 : Values of 'C_z' Corresponding to 'ΔW' and 'ΔV'

	± 2%	± 4%	± 6%	± 8%	± 10%
ΔW	263.8	425.6	796.6	1068.2	1616.7
ΔV	.293e-4	.594e-4	.89e-4	1.49e-4	1.49e-4
C_z	888e4	716e4	894e4	717e4	1088e4

centre of pressure which corresponds to the centre of pressure which corresponds to the pivot point is a function of the film ratio.

REYNOLDS EQUATION

The analysis of hydrodynamic thrust bearings have predominantly been based on the Reynolds equation for the pressure distribution. With the increasing capacity of computers, numerical models have been developed including the influences of viscosity variations along and across the lubricating film. Deformation of the bearing pads due to pressure and thermal gradients was also considered. Discretization of the pad is shown in Fig.2.

If only the lowest order terms are retained, these can be introduced in the continuity equation which is then integrated to give the Reynolds equation.

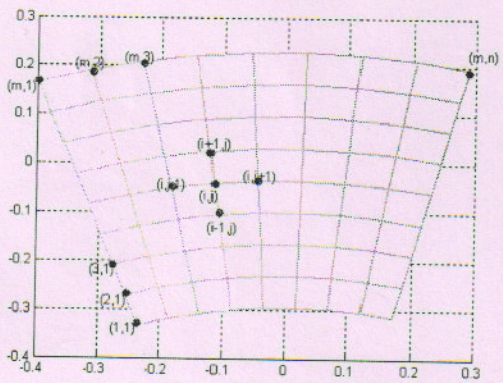

Fig. 2 Discretization of pad for Reynold's equation

The temperature of the runner along its periphery varies much less than the temperature in the stationary parts. The 'flash' temperature of the runner varies by less then 1 "C and the temperature along thrust pad rises by 15 to 20^{0}C as in [3]. Values of viscosity so obtained from the temperature field in the oil film are substituted in the Reynolds equation, to determine the pressure field. In load estimation the pressure 'fitting' at the edges has been made more appropriate to suit realistic conditions as in [4]

The generalized Reynolds equation for rectangular thrust segment is :

$$\frac{\partial}{\partial x}\left[F_2\frac{\partial p}{\partial x}\right]+\frac{\partial}{\partial y}\left[F_2\frac{\partial p}{\partial y}\right]=\frac{\partial}{\partial y}\left[\frac{F_3}{F_0}U\right] \qquad \ldots. (1)$$

F_0, F_2 and F_3 are the viscosity integrals with units of m^2. sec/kg, m.sec and sec respectively. Neglecting variation of viscosity across the thickness of the film, better numerical accuracy can be obtained for the Reynolds equation for a sector-shaped thrust segment, if all the first derivative terms in the equation are converted in to second derivative terms. For this, the following procedure is adopted. Consider,

$$\frac{\partial^2}{\partial R^2}\left[\frac{RH^3P}{\bar{\mu}}\right]=\frac{\partial}{\partial R}\left[\frac{\partial}{\partial R}\left[\frac{RH^3P}{\bar{\mu}}\right]\right]$$

$$=\frac{\partial}{\partial R}\left[\frac{RH^3}{\bar{\mu}}\frac{\partial P}{\partial R}+P\frac{\partial}{\partial R}\left[\frac{RH^3}{\bar{\mu}}\right]\right]$$

$$=\frac{RH^3}{\bar{\mu}}\frac{\partial^2 P}{\partial R^2}+2\frac{\partial P}{\partial R}\frac{\partial}{\partial R}\left[\frac{RH^3}{\bar{\mu}}\right]+P\frac{\partial^2}{\partial R^2}\left[\frac{RH^3}{\bar{\mu}}\right]$$

$$2\frac{\partial P}{\partial R}\frac{\partial}{\partial R}\left[\frac{RH^3}{\bar{\mu}}\right]=\frac{\partial^2}{\partial R^2}\left[\frac{RH^3P}{\bar{\mu}}\right]-\frac{RH^3}{\bar{\mu}}\frac{\partial^2 P}{\partial R^2}-P\left[\frac{RH^3}{\bar{\mu}}\right]\ldots \qquad (2)$$

Also,

$$\frac{\partial^2}{\partial\bar{\theta}^2}\left[\frac{PH^3}{\bar{\mu}}\right]=\frac{\partial}{\partial\bar{\theta}}\left[\frac{\partial}{\partial\bar{\theta}}\left[\frac{PH^3}{\bar{\mu}}\right]\right]$$

$$=\frac{\partial}{\partial\bar{\theta}}\left[\frac{H^3}{\bar{\mu}}\frac{\partial P}{\partial\bar{\theta}}+P\frac{\partial}{\partial\bar{\theta}}\left[\frac{H^3}{\bar{\mu}}\right]\right]$$

$$=\frac{H^3}{\bar{\mu}}\frac{\partial^3 P}{\partial\bar{\theta}^2}+2\frac{\partial p}{\partial\bar{\theta}}\frac{\partial}{\partial\bar{\theta}}\left[\frac{H^3}{\bar{\mu}}\right]+P\frac{\partial^3}{\partial\bar{\theta}^2}\left[\frac{H^3}{\bar{\mu}}\right]$$

Or,
$$2\frac{\partial P}{\partial\bar{\theta}}\frac{\partial}{\partial\bar{\theta}}\left[\frac{H^3}{\bar{\mu}}\right]=\frac{\partial^2}{\partial\bar{\theta}^2}\left[\frac{H^3p}{\bar{\mu}}\right]-\frac{H^3}{\bar{\mu}}\frac{\partial^2 P}{\partial\bar{\theta}^2}$$
$$-P\frac{\partial^2}{\partial\bar{\theta}^2}\left[\frac{H^3}{\bar{\mu}}\right] \qquad (3)$$

Substituting the above expressions and keeping $\frac{\partial h}{\partial t}=V=(i)h_o\,(h=h_o\,H;\bar{t}=t\omega)$ in equation (3) following is obtained.

$$\frac{\partial^2}{\partial R^2}\left[\frac{RH^3p}{\bar{\mu}}\right]-\frac{RH^3}{\bar{\mu}}\frac{\partial^2 P}{\partial R^2}$$
$$-P\frac{\partial^2}{\partial R^2}\left[\frac{RH^3}{\bar{\mu}}\right]+\frac{1}{R\beta^2}\frac{\partial^2}{\partial\bar{\theta}^2}\left[\frac{H^3P}{\bar{\mu}}\right]$$
$$+\frac{1}{R\beta^2}\frac{H^3}{\bar{\mu}}\frac{\partial^2 P}{\partial\bar{\theta}^2}-P\frac{\partial^2}{\partial\bar{\theta}^2}\left[\frac{H^3}{\bar{\mu}}\right]$$
$$=12R\frac{\partial H}{\partial\bar{\theta}}+24R\beta V$$

Following assumptions are made in the analysis done herein.

1. Steady-state conditions exist in the oil film.

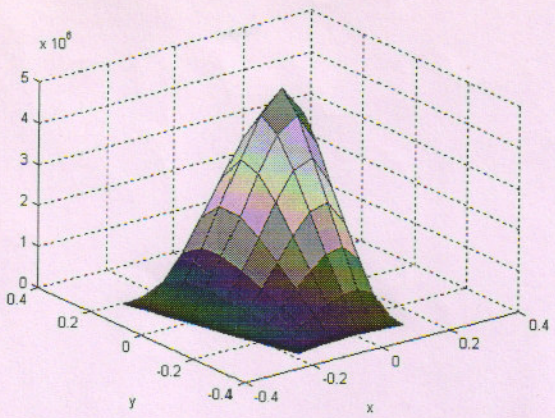

FIG. 4 3-D pressure distribution in the oil film of a flat pad, a=1.8

For the values of 'a' taken from 1.0 to 2.2 and L/B ratio from 0.7 to 1.3 the damping values are calculated. A contour plot depicting the damping values at 'a' and *'L/B'* respectively is drawn as shown in Figure.5.

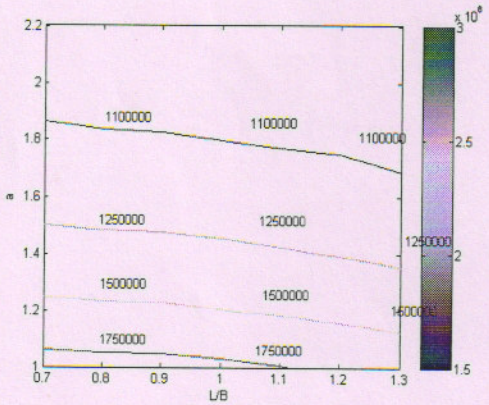

Figure 5: Damping C_z with respect to Film shape parameter *a* and *L/B* ratio

The values of W and ho are varied from 10% to -10% and the difference of these values are taken as ΔW *and* Δh_o. Table.3 shows calculated values of 'K$_z$ '

TABLE- 3 : Values of 'K_z' corresponding to 'ΔW' *and* 'Δh_o'

	± 2%	± 4%	± 6%	± 8%	±10%
ΔW	263.8	425.6	796.6	1068.2	1616.7
Δh_o	.0052	.0104	.0156	.0208	.0260
K_z	50678	40880	51011	51302	62116

Similarly sample Stiffness values for L/B ratio 0.7 to 1.3 for 'a' taken from 1.0 to 2.2 are calculated. Based on these values a contour plot as shown in Figure.6, is drawn between 'a' and 'L/B' ratio. The contours in the graph represent the stiffness values at 'a' and 'L/B' respectively. The colour bar represents the value o stiffness at respective 'a' and 'L/B' values.

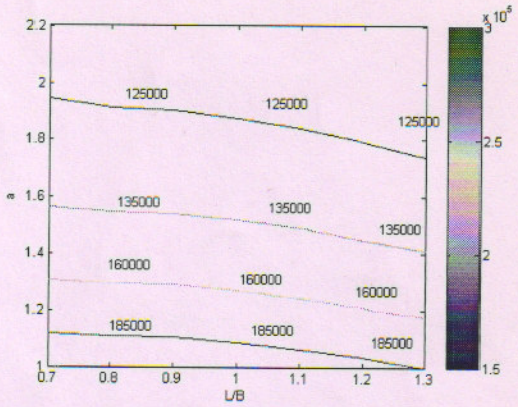

Figure.6 Stiffness K_z with respect to Film shape parameter *a* and *L/B* Ratio

The corresponding damping and stiffness values for **Yuan's dimensional parameters ,** are listed in Tables 4 and 5.

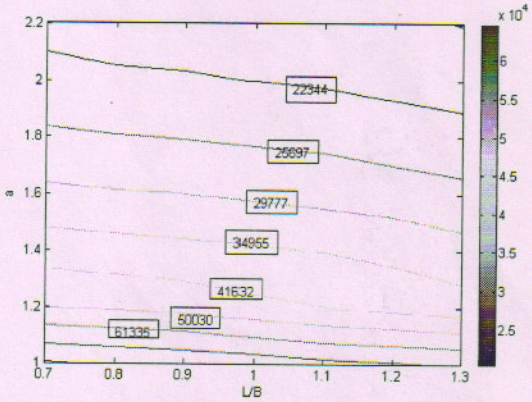

Figure.7 Yuan's Damping C_z with respect to film shape parameter *a* and *L/B* ratio

TABLE 4: Values of *'C_z'* Corresponding to *'ΔW' and 'ΔV'*

	± 2%	± 4%	± 6%	± 8%	± 10%
ΔW	20.67	41.42	62.39	83.65	105.31
ΔV	.00034	.00068	.001011	.00135	.0051
C_z	61325	61454	61711	62055	20788

Based on these values a contour plot viz. Figure 7, is made.Figure 8 shows a contours plot representing the stiffness values at 'a' and 'L/B' respectively.

TABLE 5: Values of 'K$_z$ 'corresponding to 'ΔW' and 'Δh$_o$'

	± 2%	± 4%	± 6%	± 8%	±10%
ΔW	20.67	41.42	62.39	83.65	105.3
Δh$_o$	2.7*10-7	5.3*10-7	8*10-7	1.1*10-6	1.3*10
K$_z$	77,706767	77,857143	78,57,6826	78,915094	791804

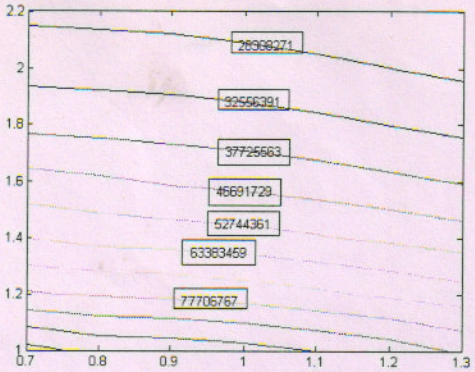

Figure. 8 Yuan's Stiffness K_z with respect to Film shape parameter a and L/B ratio

CONCLUSIONS: For the author's dimensional values the damping coefficient value at L/B = 0.7 and a=1 is 318298 N-s/m and it decreases gradually as 'a' and L/B are increased and finally at L/B = 1.3 the value of damping coefficient becomes 283685 N-s/m . The value of the stiffness at L/B = 0.7 and 'a' = 1.0 is 33619 N/m and it decreases gradually and at 'a'= 2.2 is equal to 29958 N/m . For Yuan's Dimensional values the corresponding maximum damping coefficient value is 61335 N-s/m and it decreases gradually to a minimum of 22344 N-s/m. The maximum value of the stiffness coefficients is 77706767 N/m and it decreases gradually to a minimum 28398271 N/m. The variation pattern for the damping and coefficient values for the sets of dimensions is similar, however the numerical values vary such that damping coefficient values are greater for the author's dimensions because of higher load variation and stiffness values are more for Yuan's dimensions because of lower minimum film thickness.

1. **Kettleborough, C.F.**, Procedings of ETCE2002, ASME Engineering Technology Conference on Energy, February 4-5, 2002. Houston, TX.

2. **Zhu, Q; Zhang, WJ,** Transactions of ASME, 2003, "A preliminary non linear analysis of the axial transient response of the sector shaped hydrodynamic thrust bearing rotor system", Journal of Tribology, vol.125, October, pp.854-858.

3. **Ettles, C.M.M and Anderson,** H.G., 1991, "Three – Dimensional Thermo – Elastic solutions of thrust bearings using code Marmac 1", Journal of Tribology, Transactions of the ASME, vol.112, pp.405-412.

4. **Chaturvedi, K.K., Athre, K., Nath, Y. and Biswas, S.,** 1989, "Refinement in Estimation of Load Capacity and Temperature Distribution of Pad Bearing," Proceedings of Eurotrib-89, Helisinki, Finland, June.

5. **Yuan J.H., Ferguson J.H and Medley J.B.** Spring Supported Thrust Bearings Hydroelectric Generators : Comparison of Experimental Data with Numerical Predictions, Tribology Transactions. Vol.44, pp.27-34., 2001.

CONTACT: D.V. SRIKANTH Associate Professor in Mechanical Engineering, Bharat Institute of Engineering and Technology Mangalpally Hyderabad, A.P. Email: dvsrikanth1@hotmail.com

NOMENCLATURE

a : it is the ratio of the difference between inlet film thickness and outlet film thickness to the outlet film thickness
b : length of the bearing, m
U,V : velocity along and normal to surface, m/s
W : load on bearing, N
G_P : gap between the pads,m
h_o : oil film thickness at the trailing edge, m
m : number of the nodes on the grid in radial direction
n : number of the nodes in circumferential direction coordinate along n -axis.
p : pressure in the oil film , Pa
r : radial coordinate
Δr : division on the grid along radial direction, m
r : radius of the runner,m
t : transit time ,B/U, s
B : circumferential length of the thrust segment,m
C_z : bearing damping coefficients, N-s/m
D_i : inner diameter of the thrust bearing,m
D_o : outer diameter of the thrust bearing,m

F1, : F2 ,F3 : viscosity integrals in the Reynold's equation
H : non-dimensional thickness of the oil film, h/ho
K_z : bearing stiffness coefficient , N/m
L : radial length of the thrust pad,m
N : angular speed of the runner ,rpm
P : non-dimensional pressure
P : pressure matrix in Reynold's equation
R : non-dimensional radius , r/r_o
Z : no. of pads
γ : film thickness ratio
μ : viscosity of oil , Pa.s
θ : angle from the leading edge, rad
ρ : density of oil, kg/m3
ω : angular speed of the runner, rad/s
Δθ : angular division of the grid,rad
i : index of the node in radial direction
j : index of the node in circumferential direction